Spacecraft Charging Interactive Handbook

V. A. Davis, I. Katz, M. J. Mandell and B. M. Gardner
Maxwell Technologies Systems Division, San Diego, California

Abstract

Recent spacecraft failures have brought into focus the need for increased understanding and modeling of spacecraft charging by spacecraft designers. Spacecraft charging assessments are needed for designing all geosynchronous, mid-altitude, and polar, low-earth orbit spacecraft. Under contract to the Spacecraft Environment Effects Program office at NASA/Marshall, we are developing a CD-ROM/web based multimedia interactive Spacecraft Charging Handbook with integrated, updated spacecraft charging models. This product guides the nonexpert through the appropriate analysis using the power of sophisticated charging analysis tools. It is easy to use and will be accessible over the web. The one-dimensional surface charging tools use the same physics as the NASCAP/GEO code. Over three years, six assessment modeling tools will be developed and incorporated. We have completed the Spacecraft Environment and Surface Charging tools. The Internal Charging tool is under development. During the second and third years a Three-dimensional Surface Charging tool, a Material Properties Database tool and an Auroral Charging tool will be developed.

Introduction

Under contract to the Spacecraft Environment Effects Program office at NASA/Marshall, we are developing a CD-ROM/web based multimedia interactive Spacecraft Charging Handbook with integrated, updated spacecraft charging models. This product guides the nonexpert through the appropriate analysis using the power of sophisticated charging analysis tools. Figure 1 shows the home page of the Handbook.

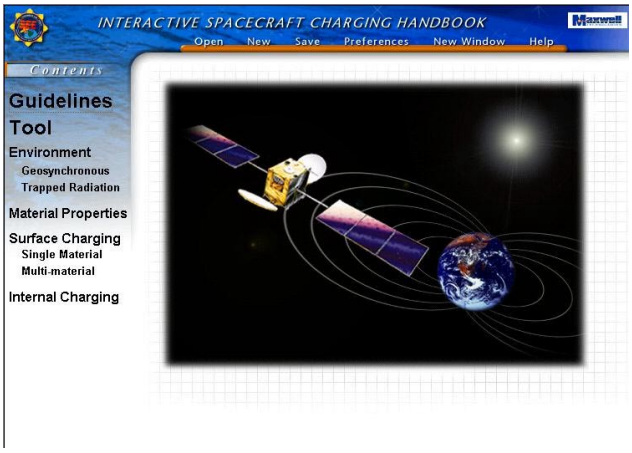

Figure 1. Home page of the SEE Spacecraft Charging Interactive Handbook.

There is a critical need for increased understanding and modeling of spacecraft charging by spacecraft designers. Spacecraft charging assessments are needed for designing all geosyn-chronous, mid-altitude, and polar, low-earth orbit spacecraft. The *1984 Design Guidelines for Assessing and Controlling Spacecraft Charging Effects* (Purvis, *et. al.*, 1984) needs extending for use with modern spacecraft. Additionally, the standard spacecraft charging code, NASCAP/GEO, is a complex tool/code to use, it does not address buried charge buildup, is limited with respect to the geometry it can model, and requires expertise to use.

This application applies the advances in interactive communications using personal computers to spacecraft design technology. It provides NASA and commercial satellite designers and managers, spacecraft charging researchers, and aerospace engineering students information on how to build satellites using advanced technologies that can survive the natural environment. Deep dielectric charging due to penetrating electrons (Wrenn, 1995) and reverse polarity differential charging on solar arrays (Katz, *et. al.*, 1998) are just two of the phenomena studied by researchers that are critically important to spacecraft design engineers.

For maximum accessibility, the Handbook is written with HTML, Javascript, and JAVA and runs within a level 4 browser, either Internet Explorer or Netscape Navigator. This choice insures that the application can run on both Windows (95 or NT 4.0) and Macintosh OS 7.5 computers, either stand alone or over the World Wide Web. The application is navigated using the table of contents on the left side of the page. There are two main sections of the Handbook: Guidelines and Tools. The Guidelines is a text document that provides guidance to the spacecraft design engineer. The Interactive Tools allow users to investigate the charging of their spacecraft. The tools have a simple intuitive design. The essential physics needed to understand and predict the charging phenomena is included in the tools.

The Design Guidelines consists of four sections: Spacecraft Charging Overview, Interactions Modeling Techniques, Spacecraft Design Guidelines, and Control and Monitoring Techniques. The Guidelines are accessed by clicking on the word “Guidelines” in the table of

contents to the left of the page. Within the Guidelines, the chapters are navigated using the bar at the bottom of the page. The document can be printed using the browser print function. Figure 2 shows the beginning of the introductory chapter.

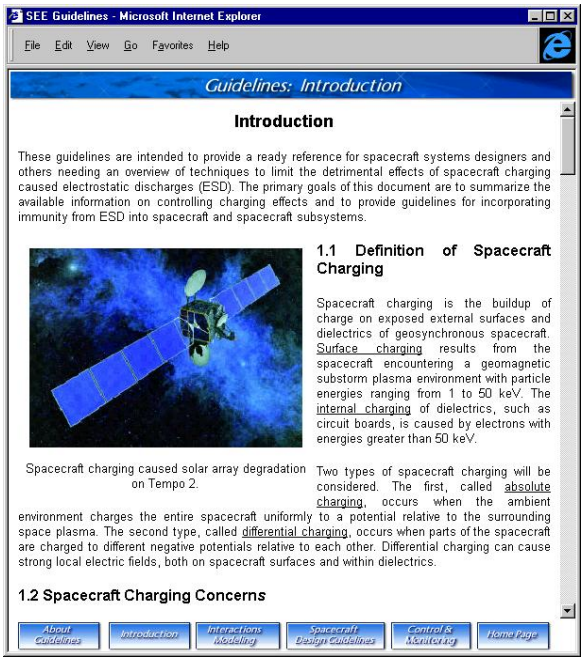

Figure 2. Beginning of the Guidelines.

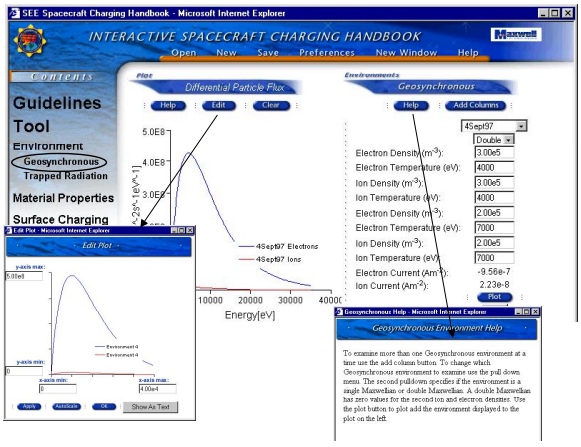

Figure 3. Illustration of several features of the tools.

Figure 3 illustrates some of the capabilities of the tools. Whenever a tool is open, there is a plot in the upper left corner of the tool area. The edit button brings up a separate window to specify the minimum and maximum axis values. This window also allows the user to specify autoscaling or to bring up a third window in which the plotted data is shown as a table. The data can then be transferred to a more sophisticated plotting package. The clear button clears the plot. Whenever the plot button (bottom right) is clicked, the appropriate data is added to the plot. The Add Column button permits the comparison of named items. The pull-down menu at the top of the column is used to specify the environment, material, or spacecraft being displayed, to create new named items, to delete named items, or to delete the column. The Help button brings up a help screen.

Environment Tools

The Geosynchronous environment tool allows the user to specify single and double Maxwellian environments. These environments are then used by the Surface Charging tools in their computations. The Trapped Radiation environment tool allows the user to define an orbit and compute the high energy electron flux from the AE-8 model. For modeling of extreme conditions, a multiplicative factor can be specified. The ten-hour average electron flux is used by the Internal Charging model. Both environment tools plot the flux as a function of particle energy.

Material Properties Tool

The Material Properties tool allows the user to specify the parameters needed to describe material interactions with the plasma environment. The dielectric constant, thickness, and conductivity are used to compute the capacitance and conductivity from the surface of the dielectric to the underlying conductor. The dose enhanced conductivity parameters and the bulk conductivity are used in computing the electric fields due to internal charging.

The electron generated secondary electron yield governs eclipse charging, so a good model is needed. The tools use the same model as NASCAP/GEO (Katz, *et al.*, 1986). The primary electron deposits energy along its path within the material. The energy loss generates secondary electrons in the material proportional to the deposited energy. The escape probability for secondary electrons depends exponentially on the depth at which they are generated. The yield for incident electrons of energy E_o and angle α is given in terms of the peak yield, the energy of the peak yield, and the four range parameters.

$$Y(E_0,\alpha) \propto \int_0^{\infty} \left(\frac{dR(x)}{dE}\right)^{-1} e^{\left(\frac{-x\cos\alpha}{\lambda}\right)} dx$$

$$R(E) = a_1 E^{b_1} + a_2 E^{b_2}$$

The mean depth of secondary emission, λ, is determined automatically from the energy for maximum yield.

The ion generated secondary yield is usually small compared with the other currents. The same physics model is used as for electron initiated secondaries. Several simplifying assumptions can be made. For ions, the stopping power is independent of path length. The peak of the yield curve is over 100 keV for most materials. The normal incidence yield can be given in terms of two parameters, Y_o, the yield extrapolated down to 1 keV and E_{max}, the energy for maximum yield.

$$Y(E) = \left(Y_o \sqrt{E}\right) \Big/ \left(1 + \frac{E}{E_{max}}\right) \text{ for } E > 10 \text{ keV}$$

The backscattered electron yield depends on the incident energy and the average atomic number, Z, of the material. Backscattered electrons account for about 10% of the total current. The normal incidence yield satisfies the following for energy greater than 10 keV.

$$(\ln Y)^2 + \left(\frac{2}{\eta}\right)(Y \times (1 - \ln Y) - 1) = 0$$

where $\eta = 0.475 Z^{0.177} - 0.4$

The photoelectron current density is provided by the user.

Charging Tools

Figure 4, the Single Material surface charging tool shows the components of the net current. As shown in the figure, for the material “Black Kapton” specified using the Material Properties tool, the environment “Worst Case” specified using the Geosynchronous environment floating potential of -11.2 kV in under 1 second. The components of the current are displayed along with the net current at 0 V and at the floating potential. tool, a backplane bias value of 0 V and 10% of the surface sunlit, the conducting material will reach a floating potential of -11.2 kV in under 1 second. The components of the current are displayed along with the net current at 0 V and at the floating potential.

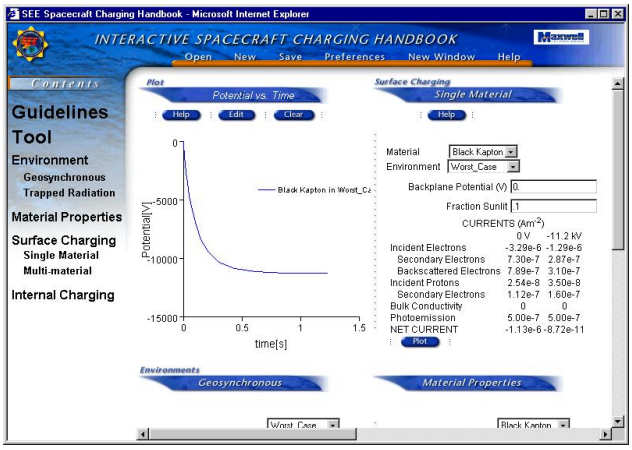

Figure 4. The Single Material surface charging tool shows the components of the net current to the surface.

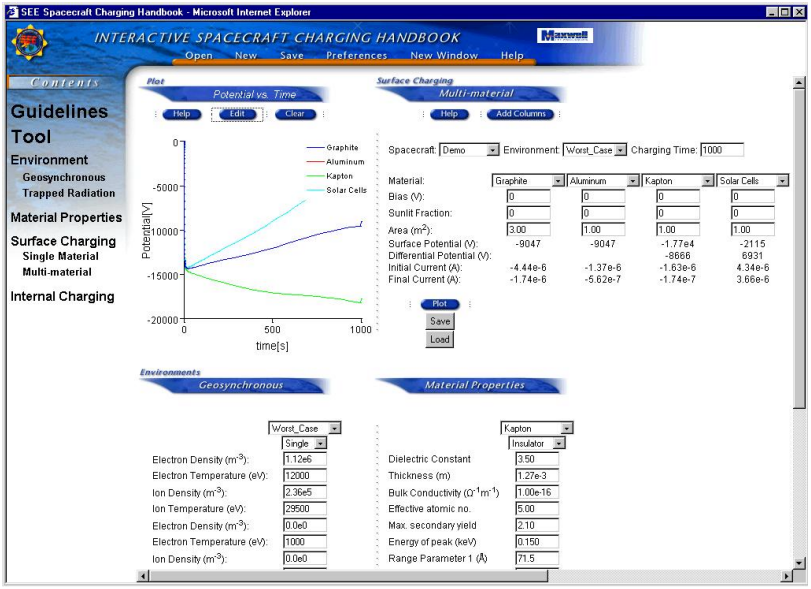

Figure 5. Multi-material charging tool.

The Multi-material charging tool shown in Figure 5 computes both overall and differential charging. Figure 6 shows a circuit diagram for a spacecraft with one insulating surface and exposed conducting surface. The widely differing capacitances of the surface to infinity, C_A and the surface to spacecraft ground, C_{AS}, make this a complex numeric problem.

$$C_{AS} = \kappa\varepsilon_0 \frac{S}{d} \approx \frac{S}{2} \times 10^{-7} \text{ Farad}$$

$$C_A \approx C_S \approx 4\pi\varepsilon_0 R$$
$$\approx R \times 10^{-10} \text{ Farad}$$

The potentials as a function of time are computed using implicit time integration of the charging equations.

$$C_A \dot{V}_A + C_{AS}(\dot{V}_A - \dot{V}_S) = I_A$$
$$-C_{AS}(\dot{V}_A - \dot{V}_S) + C_S \dot{V}_S = I_S$$

The multisurface problem is solved by linearizing the currents and inverting the matrix.

$$\mathbf{C}\,\dot{V} = I(V)$$

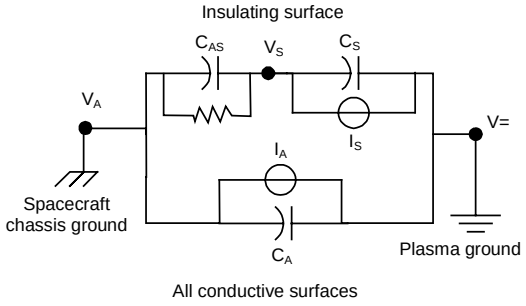

Figure 6. Circuit model of a spacecraft with one insulating surface.

Figure 7 shows a log scale plot of the surface potentials computed by the tool shown in Figure 5. The tool is able to compute the potential variation over the widely varying time scales.

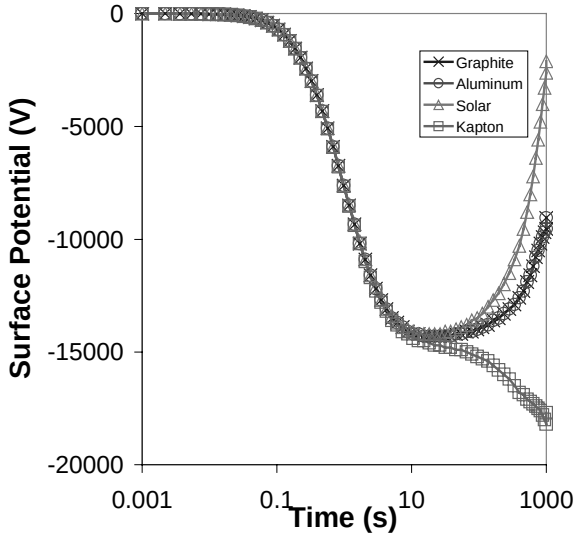

Figure 7. Surface potential for the several surfaces of a complex spacecraft..

Internal Charging Tool

The Internal Charging tool is under development in collaboration with Robb Frederickson. The tool computes the steady-state electric field internal to dielectrics for either slab or co-axial geometry. The technique is based on that described in Fredrickson et. al. (1993). The steady state current is divergenceless. The current has two parts: incident high-energy electrons and conduction. As the conduction current is proportional to the electric field, the divergence = 0 condition can be used to compute the electric field.

$$\nabla \cdot \mathbf{j} = 0$$
$$\nabla \cdot (\mathbf{j}_R + \mathbf{j}_C) = 0$$

Both bulk and dose enhanced conduction are included.

$$\mathbf{j}_C = \left(\sigma_{bulk} + k_p D^{\Delta}\right)\mathbf{E}$$

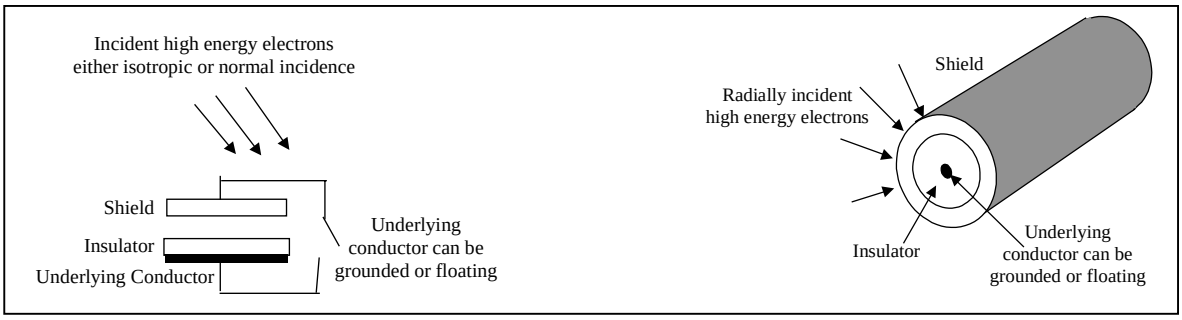

Figure 8. The internal charging tool has one-dimensional models of slab and co-axial geometries.

The charge deposition from the high energy electrons and the shielding of these electrons is computed from an analytic form based on Monte Carlo calculations (Fredrickson & Bell, 1995; Tabata, 1974). The charge deposited is the integral over the spectrum from the incident Trapped Radiation environment tool. The radiation environment is the AE-8 model with an enhancement factor to account for extrema.

$$\mathbf{j}_R(\mathbf{x}) = \int \mathbf{j}_S(\varepsilon)\, C(\mathbf{x}, \varepsilon)\, d\varepsilon$$

The charging timescale is computed from the total charge in the insulator at equilibrium and the initial charging current to the insulator.

Summary

When complete, this application will simplify the development of charging immune spacecraft. Beta testing will begin in June 1999.

References

A. R. Frederickson, S. Woolf, J. C. Garth, Model for Space Charge Evolution and Dose in Irradiated Insulators at High Electric Fields, *IEEE Trans. Nucl. Sci., 40*, 1393, 1993.

A. R. Frederickson and J. T. Bell, Analytic Approximation for Charge Current and Deposition by 0.1 to 100 MeV Electrons in Thick Slabs, *IEEE Trans. Nucl. Sci., 42*, 1910, 1995.

G. L. Wrenn, Conclusive Evidence for Internal Dielectric Charging Anomalies on Geosynchronous Communications Spacecraft, *J. of Spacecraft & Rockets, 32*, 514, 1995.

I. Katz, M. Mandell, G. Jongeward, M. S. Gussenhoven, The Importance of Accurate Secondary Electron Yields in Modeling Spacecraft Charging, *JGR, 91*, 13739, 1986.
I. Katz, V. A. Davis, D. B. Snyder, Mechanism for spacecraft charging initiated destruction of solar arrays in GEO, AIAA Paper 98-1002**,** *AIAA, Aerospace Sciences Meeting & Exhibit, 36th*, Reno, NV, Jan. 12-15, 1998.

C. K. Purvis, H. B. Garrett, A. C. Whittlesey, N. J. Stevens, *Design Guidelines for Assessing and Contolling Spacecraft Charging Effects, NASA TP-2391*, 1984.

T. Tabata, R. Ito, An Algorithm for the Energy Deposition by Fast Electrons, *Nuclear Science and Engineering, 53*, 226, 1974.